Mathematisches Forschungsinstitut Oberwolfach

Report No. 38/2006

Mini-Workshop: Anisotropic Motion Laws

Organised by
Martin Burger (Linz)
Peter Smereka (Ann Arbor)
Axel Voigt (Bonn)

August 13th – August 19th, 2006

ABSTRACT. Anisotropic motion laws play a key role in many applications ranging from materials science, biophysics to image processing. All these highly diversified disciplines have made it necessary to develop common mathematical foundations and framworks to deal with anisotropy in geometric motion. The workshop brings together leading experts from various fields to address well-posedness, accuracy, and computational efficiency of the mathematical models and algorithms.

Mathematics Subject Classification (2000): 53C44, 35K55, 37E35.

Introduction by the Organisers

During the past half-centure much activity among mathematicians, material scientists and mechanicians has been done concerning interface problems. Besides the describing equations in the bulk phases, such problems generally result in an extra interface condition. The simplest examples of such interface equations are due to Mullins and include motion by mean curvature

$$v = -\kappa \tag{1}$$

and motion by surface diffusion

$$v = \Delta_S \kappa \tag{2}$$

with v the scalar normal velocity, κ the mean curvature of the interface and Δ_S the surface Laplacian. Due to recent technolocical trents especially in semiconductor and bio-technology towards nanometer scale applications these problems gain more and more attention. As we approach smaller and smaller scales the influence of the interface compared to the bulk phases increases and already dominates in applications such as quantum-dot formation during epitaxial growth, electromigration

of voids in metal interconnects or motion of vesicles. To provide a theoretical imput for such applications material specific parameters concerning their anisotropy have to be considered in these equations. The goal of this workshop was to deal with the arriving theoretical and numerical difficulties by considering anisotropic interface equations.

To avoid geometrical complications associated with surfaces in three-dimensional space we describe the anisotropic equations in two space dimensions. The Mullins equations now read

$$(3) \qquad\qquad\qquad bv = -(\psi_0 + \psi_0'')\kappa$$

and

$$(4) \qquad\qquad\qquad \rho^2 v = \partial_s(L\partial_s((\psi_0 + \psi_0'')\kappa))$$

with $b = b(\theta)$ a kinetic modulus, depending on the angle θ, $\psi_0 = \psi_0(\theta)$ the free energy density, ρ the bulk density, $L = L(\theta)$ the mobility function and ∂_s the derivative with respect to the arc length. Both equations result from a free energy of the form $E = \int_\gamma \psi_0(\theta)ds$, by assuming ψ_0 to be smooth. For $\psi_0 + \psi_0''$ non-negative the two problems are well-posed. Under these assumptions the problems can be treated similarly to the isotropic case by considering the weighted curvature $(\psi_0 + \psi_0'')\kappa$ as an unknown.

If $\psi_0 + \psi_0''$ becomes negative for certain orientations, the equations (3) and (4) become backward parabolic. Free energy densities which lead to such ill-posdness are of relevance in thermal facetting during thin film growth. Following DiCarlo, Gurtin and Podiudugli one can deal with such anisotropies by allowing the free energy density $\psi = \psi(\theta, \partial_s\theta)$ to depend also on higher order terms. In the simplest form the free energy now reads $E = \int_\Gamma \psi_0(\theta) + \frac{\epsilon}{2}\kappa^2 ds$, with ϵ introducing a new length scale, which smears out corners in the equilibrium shape. The added Willmore term κ^2 can be viewed in a similar way as the gradient term in the Cahn-Hilliard theory. The resulting equations are

$$(5) \qquad\qquad\qquad bv = -(\psi_0 + \psi_0'')\kappa + \epsilon(\partial_{ss}\kappa + \kappa^3)$$

and

$$(6) \qquad\qquad\qquad \rho^2 v = \partial_s(L\partial_s((\psi_0 + \psi_0'')\kappa) - \epsilon(\partial_{ss}\kappa + \kappa^3)).$$

Only recently numerics are performed for these equations in a front-tracking, level-set and phase-field ansatz. Even if all these approaches provide reasonable results, theoretical arguments make it questionable if the added Willmore functional is enough to prevent the formation of corners during the evolution in three dimensions. Higer order term resulting from a free energy density $\psi(\theta, \partial_s\theta, \partial_{ss}\theta, \ldots)$ might be necessary to provide a smooth curvature.

A second interesting class of problem arises if ψ_0 is not smooth. In this case the geometric evolution laws can not even be written in the formulation (3) and (4) but rather have to be formulated in a way, which only contains the first derivative of ψ_0. Such anisotropies arise for crystalline materials, with facets in the equilibrium shape. Numerical approaches for geometric evolution laws with such anisotropies

have recently been considered again in a front-tracking, level-set and phase-field approach. In all approaches the idea is basically a weak formulation of the problem, which only needs the first derivative of ψ_0. Analytical results for such anisotropies are rare.

A third class of interface problems of recent interest, results from applications in surface science, where in addition to the evolution of the interface also processes, such as diffusion or decomposition on the evolving surface plays a dominant role. In addition to the evolution of the surface a PDE on the evolving surface has to be solved, which might influence its evolution. Such problems arise for example in the description of biomembranes and have only recently been proposed and numerical investigations are still rare. Theoretical results on evolution laws on evolving surfaces are still limited but definitely necessary for the development of an efficient numerical approach.

In all these classes the exact functional form of the anisotropy is not known for most materials. Only recently material specific quantities $\psi_0 + \psi_0''$ have been computed from first principles or have been derived from coarse grained atomistic models. The research on anisotropic motion laws is not restricted to mathematics, instead it is largely driven by applications. However, we believe mathematical research to play a key role in the development of the necessary theoretical and numerical approaches to deal with anisotropic motion laws and thus to be a key ingredient for many applications on nanometer length scales in materials science and biotechnology.

The focus of this workshop was to bring together the leading materials scientists, physicists and mathematicians in the field of anisotropic surface evolution. Besides the mathematical aspects of modeling, analysis and simulation of anisotropic geometric evolution laws also the connection to experimental results and ab initio computations was dealt with to drive the recent theoretical developments on anisotropic geometric evolution laws into a direction which is relevant for a large variety of applications. Ab initio calculations of material specific anisotropy functions and measurements of equilibrium shapes on a nanometer scale are only recently available and the discussion on the right functional form of the anisotropy is still controversary.

The workshop started with introductory lectures on classical isotropic geometric evolution laws, such as mean curvature flow, surface diffusion and Willmore flow in which analytical as well as numerical results have be discussed. After introducing the different sources of anisotropy in these models the main part of the workshop started with recent results on higher order evolution laws, resulting from curvature dependent surface free energies. Front tracking, phase field and level set methods were discussed for these equations. Further talks dealt with crystalline anisotropies and their analytical and numerical treatment in geometric evolution laws as well as work on evolution laws including species transport along the surface. In the last part of the workshop several applications from image processing, materials science and biophysics were discussed.

Mini-Workshop: Anisotropic Motion Laws

Table of Contents

Abstracts

On singular perturbations of some partial differential equations
Giovanni Bellettini

It is known that mean curvature flow of the boundary of a smooth bounded open subset of $\mathbb{R}^n$ develops singularities at finite time: the simplest example is when $n = 2$, for which the singularity is the disappearence of the curve, i.e., when the curve reduces to a point [5]. It is therefore reasonable to regularize the problem with a sequence of problems which admit a global solution and then to try to pass to the limit as the regularization parameter converges to zero. One possible regularization consists in adding, at the level of the energy functionals, an higher order term. For the case of immersed curves γ, the regularized functional reads as

$$\mathcal{G}_\epsilon(\gamma) := \int_\gamma (1 + \epsilon \kappa^2) \, ds,$$

where s is the arclength parameter, κ is the curvature of the curve and $0 < \epsilon << 1$. The gradient flow of $\mathcal{G}_\epsilon$ becomes

$$(1) \qquad \frac{\partial \gamma}{\partial t} = \left(\kappa - 2\epsilon \partial_s^2 \kappa - \epsilon \kappa^3 \right) \nu,$$

where ν is a suitable choice of the normal unit vector to the curve. The first result, proved in the joint paper [1] with C. Mantegazza (Scuola Normale Superiore, Pisa) and M. Novaga (University of Pisa), is the convergence of solutions to (1) to the original curvature flow as $\epsilon \to 0$, before the shrinking time. A similar result holds (before singularities) for the mean curvature flow of an n-dimensional manifold M flowing by mean curvature in $\mathbb{R}^{n+m}$, $n \geq 1$, $m \geq 1$. In this case we add to the area functional a term similar to $\epsilon \int_M |\nabla^{k-3} B|^2$, where B is the second fundamental form of M and $k > [n/2] + 2$ (see [1] for all details). Such a term guarantees the global existence of the geometric flow for positive ϵ. Note that, in the case of surfaces flowing in $\mathbb{R}^3$, the regularizing equation is of order six. The statement of the convergence result is the following.

Let $\varphi_0 : M \to \mathbb{R}^{n+m}$ be a smooth immersion of a compact n–dimensional manifold without boundary. Let $T_{\mathrm{sing}} > 0$ be the first singularity time of the mean curvature flow $\varphi : M \times [0, T_{\mathrm{sing}}) \to \mathbb{R}^{n+m}$ of M. For any $\epsilon > 0$ let $\varphi^\epsilon : M \times [0, +\infty) \to \mathbb{R}^{n+m}$ be the flows associated with the regularized functionals, all starting from the same initial immersion φ_0. Then the maps φ^ϵ converge locally in $C^\infty(M \times [0, T_{\mathrm{sing}}))$ to the map φ, as $\epsilon \to 0$.

Another type of singular perturbation concerns the so-called Perona-Malik equation [6]. Such an equation is of forward-backward parabolic type, depending on the values of the gradient of the solution. In one space dimension, it arises as the gradient flow of the nonconvex functional

$$\frac{1}{2} \int_{(0,1)} \phi(u_x) \, dx,$$

where $\phi(p) = \log(1 + p^2)$, and reads as

$$u_t = (\phi'(u_x))_x.$$

Such an equation provides an interesting (and peculiar) example of gradient flow of nonconvex energies: other examples can be obtained by taking $\phi(p) = (1 - p^2)^2$, or considering the geometric evolutions of curves by the gradient flow of the energy

$$\int_\gamma \varphi(\nu) \, ds,$$

where $\varphi : \mathbb{R}^2 \to \mathbb{R}$ is one-homogeneous and $\{\varphi \le 1\}$ is a smooth compact even nonconvex set containing the origin in its interior.

One possible way of regularizing the Perona-Malik equation is via the fourth order problems

$$(2) \qquad\qquad u_t = \phi''(u_x)u_{xx} - \epsilon u_{xxxx},$$

see also [7] in case of a different equation, and [4]. We have discussed some theoretical and numerical results concerning the behaviour of solutions u_ϵ to (2) for small $\epsilon > 0$, such as the formation of microstructures for short times, and the coarsening for large times. Such results have been obtained in collaboration with G. Fusco (University of l'Aquila) and N. Guglielmi (University of l'Aquila), see [2], [3].

REFERENCES

[1]   G. Bellettini, C. Mantegazza, M. Novaga: *Singular perturbations of mean curvature flow*, math.AP/0407325, 2004, submitted.

[2]   G. Bellettini and G. Fusco, *The Γ-limit and the related gradient flow for singular perturbation functionals of Perona-Malik type*, Preprint Centro De Giorgi, 2004, submitted.

[3]   G. Bellettini, G. Fusco, N. Guglielmi, *A concept of solution for forward-backward equations of the form $u_t = \frac{1}{2}(\phi'(u_x))_x$ and numerical experiments for the singular perturbation $u_t = -\epsilon^2 u_{xxxx} + \frac{1}{2}(\phi'(u_x))_x$*, Discrete Contin. Dyn. Syst., to appear.

[4]   E. De Giorgi, *Congetture riguardanti alcuni problemi di evoluzione*. Duke Math. J. **81** (1995), 255-268.

[5]   M.A. Grayson, *The heat equation shrinks embedded plane curves to round points*, J. Differential Geom., **26** (1987), 285–314.

[6]   P. Perona and J. Malik, *Scale space and edge detection using anisotropic diffusion*, IEEE Trans. Pattern Anal. Mach. Intell. **12** (1990), 629–639.

[7]   M. Slemrod, *Dynamics of measured valued solutions to a backward-forward heat equation*, J. Dyn. Differential Equations **3** (1991), 614–622.

Cartoon Extraction Based on Anisotropic Image Classification

Benjamin Berkels

(joint work with Martin Burger, Marc Droske, Oliver Nemitz, Martin Rumpf)

We propose a new approach for the extraction of cartoons from 2D aerial images. An already classical approach for cartoon extracton is the Rudin-Osher-Fatemi model [5]. This method and its variants are well-suitable to restore sharp edge contours. But at corners formed by edges they come along with a significant rounding artifact. In particular for images characterized by rectangular shapes this hampers the identification of structures and destroys a proper cartoon representation.

We assume, that the given possibly noisy and locally destroyed image contains primarily structures with straight edges and corners with right angles. Furthermore, we assume that the orientation of these structures varies in space. In particular we do not fix an orientation a priori. The aim is now to extract a cartoon representation of image shapes, while preserving or even enhancing edges *and* sharp corners. This extraction can also be regarded as an image restoration technique. As a prototype application we consider aerial images of city zones.

Here we propose a joint classification of image anisotropies and a discontinuity-preserving denoising model based on an anisotropic variant of the ROF-model [2].

A Variational Approach. Let us first state the main goals of the model. For the restored image u it is desirable to preserve the functional features of the signal such as discontinuities of codimension one (e.g. edges for twodimensional images) and at the same time geometric features, such as the shape of the level sets of the original signal, with its characteristics of codimension two. For the non-texture part of images it can often be assumed that in many areas the anisotropic structure does not vary strongly in space. Hence, we aim not only at the preservation of geometric features but also at restoration in smaller areas, where strong corruption of the morphology can still be recovered by the shape information in the vicinity.

Since it is well known that the l_1-norm as anisotropy will restore right angles aligned to the coordinate axes we use a rotated l_1-norm as anisotropy and introduce a free parameter α, which represents the angle of the rotation. This leads to the energy

$$E[u, \alpha] := \frac{\lambda}{s} \int_\Omega |u - u_0|^s \, \mathrm{d}x + \int_\Omega |M(\alpha)\nabla u|_1 \, \mathrm{d}x + \int_\Omega \frac{1}{2} \left(\mu_1 |\nabla \alpha|^2 + \mu_2 |\Delta \alpha|^2\right) \, \mathrm{d}x,$$

where $1 \leq s < \infty$ and $M(\alpha)$ denotes the orthogonal matrix for a rotation by $-\alpha$. We consider a higher order regularization energy for α, because the focus of the proposed restoration method is the treatment of corners, which are co-dimension two objects.

Please note that we do not rely on *estimated* shape classification, which is used to specify a given anisotropy a priori like previous models [3].
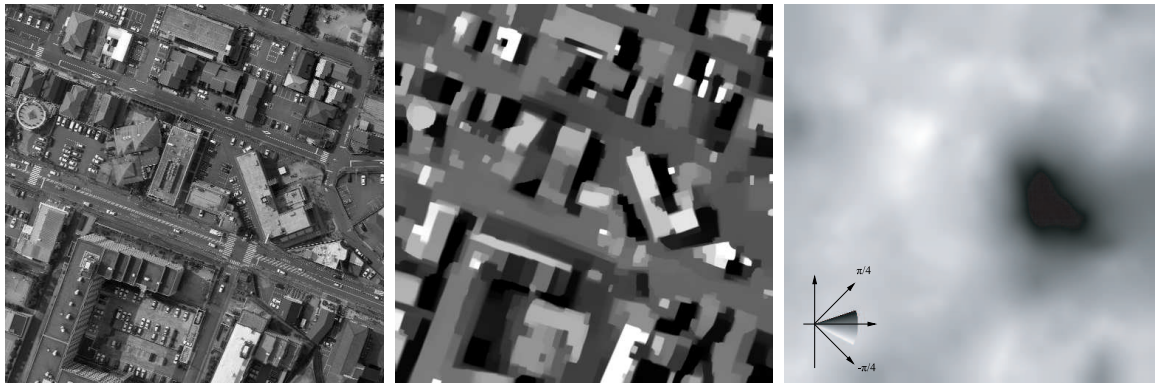
FIGURE 1. Original image (left), computed cartoon (middle) and classification (right).

Postprocessing by Bregman iteration. The coefficients have to be chosen adequately to balance the fidelity energy and the anisotropic length functional in such a way that the sharpening of edges is indeed energetically more preferable than just keeping destroyed edges in their initial shape. This leads to a rather small coefficient for the fidelity term resulting in a significant loss of contrast. To compensate for this loss, we proceed iteratively for with the minimization problems resulting from the following *Bregman* iteration [4]:

$$(u^{k+1}, \alpha^{k+1}) := \arg\min_{(u,\alpha)} \left\{ \int_\Omega |M(\alpha)\nabla u|_{1,\delta}\, \mathrm{d}x + \frac{\lambda}{2} \int_\Omega (u_0 + v^k - u)^2\, \mathrm{d}x + E_\alpha[\alpha] \right\},$$

where $v^{k+1} := v^k + u_0 - u^{k+1}$, $v^0 := 0$, $k = 0, \ldots$. Thereby we retain high contrast already in the early stage of the iteration.

Numerical implementation. We employ a time discrete gradient flow with metric

$$g(w_1, w_2) = (w_1, w_2)_{L^2} + \frac{\sigma^2}{2} (\nabla w_1, \nabla w_2)_{L^2},$$

where $w_i = (u_i, \alpha_i)$ to simultaneously minimize the regularized energy for u and α in each Bregman iteration (cf. [1]). The step-size τ of the gradient flow is controlled by the Armijo-rule.

Therefor we need the gradient of the energy and so we have to regularize the corner singularities in the anisotropy. Thus, we replace the l_1-norm by its regularized version $|x|_{1,\delta} = |x_1|_\delta + |x_2|_\delta$ with $|z|_\delta = \sqrt{|z|^2 + \delta^2}$.

Further we consider a uniform rectangular mesh $\mathcal{C}$ covering the whole image domain Ω and use a standard bilinear Lagrange finite element space. The integrals $\int_\Omega vw\, \mathrm{d}x$ and $\int_\Omega \nabla\xi \cdot \nabla\vartheta\, \mathrm{d}x$ result in the usual mass (M) and stiffness (L) matrices. Since we deal with piecewise bilinear finite elements, we introduce a second unknown $w = -\Delta\alpha$ and write $\int_\Omega \Delta\alpha\Delta\vartheta = \int_\Omega \nabla w \cdot \nabla\vartheta$, which leads to the matrix $LM^{-1}L$.

Mathematics (Austrian Academy of Sciences). The data is courtesy Aerowest GmbH and Vexcel Corporation.

REFERENCES

[1] U. Clarenz, G. Dziuk, M. Rumpf. On generalized mean curvature flow in surface processing. In H. Karcher and S. Hildebrandt, editors, *Geometric analysis and nonlinear partial differential equations*, pages 217–248. Springer, 2003.
[2] S. Esedoḡlu, S.J. Osher. Decomposition of images by the anisotropic Rudin-Osher-Fatemi model. *Comm. Pure Appl. Math.*, 57(12):1609–1626, 2004.
[3] O. Nemitz, M. Rumpf, T. Tasdizen, R. Whitaker. Anisotropic curvature motion for structure enhancing smoothing of 3D MR angiography data. May 2006. submitted to Journal of Mathematical Imaging and Vision.
[4] S. J. Osher, M. Burger, D. Goldfarb, J. Xu, W. Yin. An iterative regularization method for total variation-based image restoration. *SIAM Multiscale, Modeling and Simulation*, 4(2):460–489, 2005.
[5] L. Rudin, S. Osher, E. Fatemi. Nonlinear total variation based noise-removal. *Physica D*, 60:259–268, 1992.

Strongly Anisotropic Motion Laws, Curvature Regularization, and Time Discretization

MARTIN BURGER

(joint work with Frank Haußer, Christina Stöcker, Axel Voigt)

In this talk we discuss the numerical solution of anisotropic motion laws with surface energies of the form

$$(1) \qquad E[\Gamma] = \int_\Gamma \left(\gamma_0(\vec{n}) + \frac{\epsilon}{2} H^2 \right) \, d\mathcal{H}^{N-1},$$

where $\vec{n}$ denotes the unit outer normal and H the mean curvature of the curve or surface Γ. Particular attention is paid to the strongly anisotropic case with γ_0 (respectively its one-homogeneous extension) being nonconvex and ϵ being small. In this case, the dynamics by attachment-detachment kinetics (fourth order) and surface diffusion (sixth order) become like a geometric spinodal decomposition. After a fast initial time scale, the surface facets (with rounded corners) and a coarsening among the facets appears on different time scales. The behaviour is illustrated in Figure 1, showing the initial value and time steps 1, 5, 30, 300, and 580 (see [3] for detailed parameter settings).
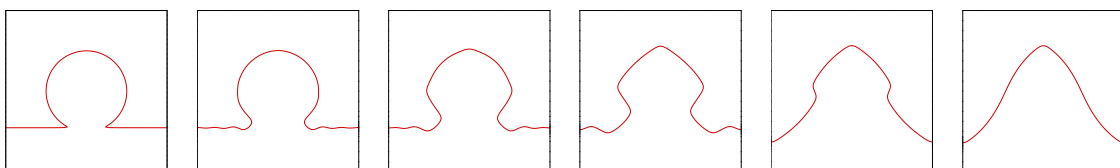

FIGURE 1. Shape change of an Ω-shape to equilibrium by strongly anisotropic surface diffusion, see [3].

The complex behaviour caused by the strong nonlinearities and the high order of the underlying evolution equations is a strong challenge to computational schemes. As usual the first issue is the choice of a shape representation, in the present application graph-like representations (cf. [2]), parametric curves (cf. [6]), as well as level set methods have been used (cf. [3]). Obviously the latter allows for most flexibility concerning the topology of the evolving shapes, but also has to be dealt with most carefully due to missing maximum principles in the high-order evolution equations. The proposed approach is therefore to compute the evolution on a grid locally refined around the zero level set and avoid numerical influence of other level sets by redistancing after small time steps (cf. [3]).

In any case of shape representation, particular attention has to be paid to suitable time discretizations. Therefore, the second part of the talk was concernced with the design of stable semi-implicit time discretizations in an automated way based on metric gradient flow formulations (cf. [1]). The natural implicit time discretization for such gradient flows is

$$\Gamma(t) = \arg \min_{\Gamma \in \mathcal{M}} \left\{ \frac{1}{2\tau} d(\Gamma, \Gamma(t - \tau))^2 + E[\Gamma] \right\}$$

where $\mathcal{M}$ is a manifold of shapes, equipped with a metric d. Both attachment-detachment kinetics and surface diffusion can be formulated in this way with the same energy functional by adapting the choice of the metric (cf. [4]). From an abstract point of view, each dissipative discretization scheme for the metric gradient flows can be written in the form

$$\Gamma_h(t) = \arg \min_{\Gamma \in \mathcal{M}_h} \left\{ \frac{1}{2\tau} d_h(\Gamma, \Gamma_h(t - \tau))^2 + E_h[\Gamma] \right\},$$

with a discretized manifold $\mathcal{M}_h$ (depending on the shape representation) and approximations of metric and energy. We show that stable semi-implicit schemes can be obtained by quadratic approximations of metric and energy, leading only to linear systems to be solved in each time steps. The crucial step in order to gain stability is a majorization property of the approximate energy E_h with respect to the energy E, which leads to energy dissipation. The computed energy dissipation in the strongly anisotropic surface diffusion (in the case of the above Ω-shape) is shown in Figure 2. Besides the schemes used in [2, 3] most known stable schemes for geometric evolution equations can be put into this framework and automatized, e.g. explicit schemes with time step restrictions, the schemes constructed by Deckelnick and Dziuk [5] for weighted mean curvature flow and surface diffusion, as well as the schemes presented by Robert Nürnberg (parametric) and Peter Smereka (level set) in this workshop.

References

[1] L. Ambrosio, N. Gigli, G. Savare, *Gradient Flows in Metric Spaces and in the Space of Probability Measures*, Birkhäuser, Basel, 2005.
[2] M. Burger, *Numerical simulation of anisotropic surface diffusion with curvature-dependent energy*, J. Comput. Phys. **203** (2005), 602-625.
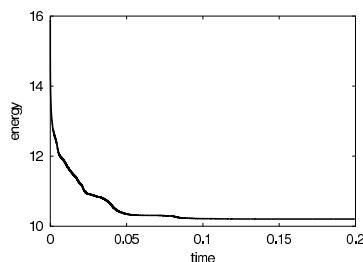
FIGURE 2. Energy dissipation during the shape change of an Ω-shape, see [3].

[3] M. Burger, F. Haußer, C. Stöcker, A. Voigt, *A level set approach to anistropic flows with curvature regularization*, Preprint (2006), submitted.
[4] W.C. Carter, J.E. Taylor, J.W. Cahn, *Variational methods for microstructural evolution*, JOM **49** (1997), 30-36.
[5] K.Deckelnick, G.Dziuk, *A fully discrete numerical scheme for weighted mean curvature flow*, Numer. Math. **91** (2002), 423-452.
[6] F. Haußer, A. Voigt, *A discrete scheme for regularized anisotropic surface diffusion, a sixth order geometric evolution equation*, Interf. Free Bound. **7** (2005), 1-17.

Moving Boundary Applications in Process and Interconnect TCAD

HAJDIN CERIC

(joint work with Johann Cervenka, Erasmus Langer, Siegfried Selberherr)

Modern Technology Computer Aided Design (TCAD) applications demand mathematical descriptions of physical phenomena, which are both accurate and suitable for numerical implementation. In the case of an evolving surface, mathematical models include material exchange between surface and surrounding phases and, at the same time, material transport along the surfaces. Stress phenomena often play a crucial part in the formation and evolution of free surfaces and, therefore, a model framework must also consistently include mechanical sub-models. For some applications, such as simulation of crystalline texture evolution, it is also necessary to extend the single surface models towards surface models for multiphase systems.

The numerical handling of mathematical models has to produce computationally efficient algorithms with reasonable demand on computer resources. Convergence and stability conditions should not impose strong restrictions on the choice of simulation domain geometries and discretization meshes.

The most general form of an evolving surface normal speed $v_n(\mathbf{r})$ used in TCAD applications is

$$(1) \qquad v_n(\mathbf{r}) = \nabla_s(D(\mathbf{r})(q\mathbf{E}(\mathbf{r}) + \gamma_s\Omega\nabla_s\kappa) \cdot \mathbf{t}) + F(\mathbf{r}).$$

The first term corresponds to surface material transport which is driven by the external field ($\mathbf{E}(\mathbf{r})$) and the curvature gradient ($\nabla_s\kappa$). $D(\mathbf{r})$ is the anisotropic surface diffusivity, $\mathbf{t}$ is the unit vector tangential to the surface, γ_s is the surface

energy, Ω is the volume of an atom, q is the effective charge, and $F(\mathbf{r})$ is the general speed function depending on the material exchange with the surrounding phases. Equation (1) describes the motion of a sharp interface, which implies that any utilized numerical approach has to deal with spatial discretization of an evolving surface. The surface is described by specifying a usually large number of points on it. Over the time the phase surface evolves and changes its morphology and even more points may be required to accurately describe it. Such techniques are quite complicated to implement and also tend to have rather poor numerical stability.

For the investigation of electromigration induced void evolution we have applied a modified Chan-Hilliard equation [2, 1]. Here, the dominant material transport is electromigration and self-diffusion at the void surface. A material exchange between a metal bulk and the void surface is neglected so that the sharp interface formulation of the moving boundary given by (1) can be simplified by setting $F(\mathbf{r}) \equiv 0$. The Chan-Hilliard theory enables a representation of an evolving void surface as interface between two phases. Both phases are defined by values of an order parameter ϕ, which takes the value $+1$ in the metal and the value -1 in the void area. This interface between phases is not sharp but has a finite width where ϕ takes values between -1 and $+1$. The phase field interpretation of the model equation (1) is

$$(2) \qquad \frac{\partial \phi}{\partial t} = \frac{2D}{\epsilon \pi} \nabla \cdot (\nabla \mu + q\mathbf{E}),$$

$$(3) \qquad \mu = \frac{4\Omega \gamma_s}{\epsilon \pi} (f'(\phi) - \epsilon^2 \Delta \phi).$$

where μ is the chemical potential, $f(\phi)$ is the double obstacle potential as defined in [1], and ϵ is a parameter controlling the void-metal interface width. The equation system (2),(3) is solved by means of a finite element method in combination with adaptive mesh refinement [2]. The described approach is utilized for investigation of void behavior in the vicinity of high gradient electrical fields and void collision with a barrier layer [2].

During deposition or etching in process technology a material is added or removed from the free evolving surface, respectively. A general assumption is low adatom mobility so that the first term in (1) can be neglected and the surface evolution is defined by the simple relation $v_n(\mathbf{r}) = F(\mathbf{r})$. The speed function is generally related to properties of the reactor, where the deposition or etching process takes place. In this case it is convenient for simulation to apply the Level Set method [4]. This approach is presented considering as an example the etching of sacrificial silicon dioxide (SiO_2) layer by hydrofluoric acid (HF).
The chemical reaction on the surface of the sacrificial layer is [3]

$$(4) \qquad 6\,HF + SiO_2 \ \longleftrightarrow \ H_2SiF_6 + 2H_2O.$$
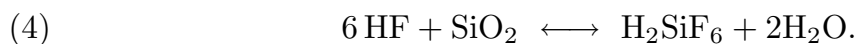
The transport of the etching agent (HF) occurs via linear diffusion,

$$(5) \qquad \frac{\partial C_{HF}}{\partial t} = \nabla \cdot (D\nabla C_{HF}),$$

with the boundary conditions $C(0,t) = C_b$ where the etching agent enters the simulation domain. On the interface between the sacrificial layer surface and the etch medium (etching front) the following boundary relationships hold

$$\begin{aligned} C_{\mathrm{HF}}(\mathbf{r}, t) &= C_s, \\ \frac{\partial C_{\mathrm{HF}}}{\partial \mathbf{n}} &= J_{\mathrm{HF}} = k_1 C_s + k_2 C_s^2, \end{aligned} \tag{6}$$

for $t > 0$. $\mathbf{r}$ is the position vector belonging to the etching front and $\mathbf{n}$ is the normal vector.

The geometrical shape of the etching front is described by the Level Set function ϕ. The zero iso-surface is equivalent to the geometrical interface. The Level Set function has a same meaning as order parameter in Chan-Hilliard theory and therefore the same symbol ϕ is used. For a given speed function F the governing equation of the Level Set is [4],

$$\frac{\partial \phi}{\partial t} + F\|\nabla\phi\| = 0. \tag{7}$$

On the basis of equation (4) we obtain the characteristic speed function for sacrificial etching at the etching front,

$$F = -\frac{\Delta\delta}{\Delta t} = -6\, J_{\mathrm{HF}} \frac{1}{\rho_{\mathrm{SiO_2}}}, \tag{8}$$

where $\Delta\delta$ is a small displacement of the etch front during time step Δt. This locally determined speed function is extended to the whole simulation domain in order to solve equation (7). The relationships (6) can now be rewritten to include the Level Set description of the etching front. Introducing a parameterized surface description $\mathbf{r}_\phi = \mathbf{r}_\phi(\alpha_1, \alpha_2)$, where $\alpha_1, \alpha_2 \in R$ and are chosen so that $\phi(\mathbf{r}_\phi) = 0$, leads to

$$\begin{aligned} C_{\mathrm{HF}}(\mathbf{r}_\phi, t) &= C_s, \\ \frac{1}{\|\nabla\phi\|}\nabla C_{\mathrm{HF}} \cdot \nabla\phi\Big|_{\mathbf{r}=\mathbf{r}_\phi} &= J_{\mathrm{HF}} = k_1 C_s + k_2 C_s^2. \end{aligned} \tag{9}$$

By means of equations (5) and (7) and the interfacial conditions (9) the moving boundary problem is well-defined. Simulations based on this model are used for investigations of a sacrificial layer profile in dependence on an etch agent distribution.

References

[1] J. Blowey and C. Elliott. The Chan-Hilliard gradient theory for phase separation with non-smooth free energy, part II: Numerical analysis. *European Journal of Applied Mathematics*, 3:147–179, 1992.

[2] H. Ceric and S. Selberherr. An adaptive grid approach for the simulation of electromigration induced void migration. *Proceedings SISPAD Conference*, pages 253–257, 2002.

[3] J. Liu, Y. C. Tai, J. Lee, K. C. Pong, Y. Zohar, and C. M. Ho. In Situ Monitoring and Universal Modeling of Sacrificial PSG Etching Using Hydrofluoric Acid. *Proceedings An Investigation of Micro Structures, Sensors, Actuators, Machines and Systems Conference*, pages 7–10, 1993.
[4] J. A. Sethian. *Level Set Methods and Fast Marching Methods*. Cambridge University Press, 1999.

A finite element method for anisotropic mean curvature flow of graphs

Klaus Deckelnick

(joint work with Gerhard Dziuk)

We consider a family of hypersurfaces $\Gamma_t \subset \mathbb{R}^{n+1}$, $0 \leq t < T$, which evolve according to the weighted mean curvature flow

$$(1) \qquad\qquad V = -H_\gamma \qquad \text{on } \Gamma_t.$$

Here V is the normal velocity of Γ_t and H_γ denotes its anisotropic mean curvature with respect to the smooth, positive, convex and 1–homogeneous weight function $\gamma : \mathbb{R}^{n+1} \setminus \{0\} \to \mathbb{R}$. The law (1) can be interpreted as the L^2–gradient flow of the weighted area $\int_\Gamma \gamma(\nu) dA$, where ν denotes the unit normal to Γ.

Let us assume that the surfaces Γ_t are graphs over some base domain $\Omega \subset \mathbb{R}^n$, so that $\Gamma(t) = \{(x, u(x,t)) \mid x \in \Omega\}$ with the orientation given by $\nu = \frac{(\nabla u, -1)}{\sqrt{1+|\nabla u|^2}}$. The evolution law (1) then translates into the following PDE for the height function u:

$$(2) \qquad u_t - \sqrt{1+|\nabla u|^2} \sum_{i,j=1}^{n} \gamma_{p_i p_j}(\nabla u, -1) u_{x_i x_j} = 0 \qquad \text{in } \Omega \times (0,T),$$

to which we add the following boundary and initial conditions

$$(3) \qquad\qquad u = g \quad \text{on } \partial\Omega \times (0,T),$$

$$(4) \qquad\qquad u(\cdot, 0) = u_0 \quad \text{in } \Omega.$$

Assuming that γ is strictly convex, i.e.

$$\exists \gamma_0 > 0 \quad D^2\gamma(p)q \cdot q \geq \gamma_0 |q|^2 \qquad \forall p, q \in \mathbb{R}^{n+1}, |p| = 1, p \cdot q = 0$$

an existence and uniqueness result for the initial–boundary value problem (2)–(4) follows from results due to [9] under suitable conditions on γ, u_0, g and $\partial\Omega$ (see also [2]). The variational form of (2),

$$\int_\Omega \frac{u_t \varphi}{\sqrt{1+|\nabla u|^2}} + \sum_{i=1}^{n} \int_\Omega \gamma_{p_i}(\nabla u, -1) \varphi_{x_i} = 0 \qquad \forall \varphi \in H_0^1(\Omega), 0 \leq t \leq T$$

forms the basis for discretizing the problem in space. Let $\mathcal{T}_h$ be a regular family of triangulations of Ω, $\Omega_h = \bigcup_{S \in \mathcal{T}_h} S$ and X_h the space of linear finite elements as well as $X_{h0} := X_h \cap H_0^1(\Omega_h)$. Furthermore, let $\tau > 0$ be a time step, $t_m := m\tau$

and denote by $u_h^m \in X_h$ the approximation to $u(\cdot, t_m)$. We now introduce the
Algorithm: given $u_h^m \in X_h$, find $u_h^{m+1} \in X_h$ such that $u_h^{m+1} - I_h g \in X_{h0}$ and

$$\frac{1}{\tau} \int_{\Omega_h} \frac{(u_h^{m+1} - u_h^m)\varphi_h}{Q_h^m} + \sum_{i=1}^n \int_{\Omega_h} \gamma_{p_i}(\nabla u_h^m, -1)\varphi_{h,x_i}$$

$$+ \lambda \int_{\Omega_h} \frac{\gamma(\nu_h^m)}{Q_h^m} \nabla(u_h^{m+1} - u_h^m) \cdot \nabla\varphi_h = 0 \quad \forall \varphi_h \in X_{h0}.$$

Here I_h is the usual Lagrange interpolation operator while we also used the abbreviations $Q_h^m = \sqrt{1 + |\nabla u_h^m|^2}$ and $\nu_h^m = \frac{(\nabla u_h^m, -1)}{Q_h^m}$. Note that in each time step a linear system of equations has to be solved. Our main results are a stability estimate and an optimal error estimate for natural geometric quantities:
Theorem: Suppose that

$$\lambda \inf_{|p|=1} \gamma(p) > \frac{1}{\sqrt{5} - 1} \max\left\{ \sup_{|p|=1} |\nabla\gamma(p)|, \sup_{|p|=1} |D^2\gamma(p)| \right\}.$$

Then we have for $M \geq 1$

a) $\sum_{m=0}^{M-1} \tau \int_{\Omega_h} |V_h^m|^2 Q_h^m + \int_{\Omega_h} \gamma(\nu_h^M) Q_h^M \leq \int_{\Omega_h} \gamma(\nu_h^0) Q_h^0.$

b) There exists $\tau_0 > 0$ such that for all $0 < \tau \leq \tau_0$

$$\sum_{m=0}^{M-1} \tau \int_{\Omega \cap \Omega_h} |V(\cdot, t_m) - V_h^m|^2 Q_h^m + \max_{0 \leq m \leq M} \int_{\Omega \cap \Omega_h} |\nu(\cdot, t_m) - \nu_h^m|^2 Q_h^m \leq c(\tau^2 + h^2).$$

Here, $V(\cdot, t_m) = -\frac{u_t(\cdot, t_m)}{\sqrt{1 + |\nabla u(\cdot, t_m)|^2}}$ and $V_h^m = -\frac{(u_h^{m+1} - u_h^m)/\tau}{Q_h^m}$.

Proof. see Theorem 3.1 and Theorem 4.3 in [3].

An error analysis for a semi–discretization in space of (2)–(4) is carried out in [2]. A number of results have been obtained for the anisotropic evolution of one–dimensional graphs. The case of a nonconvex weight function γ is studied in [7]. For such a problem, numerical calculations are carried out in [6]. Analysis and numerical results for a crystalline anisotropy can be found in [5]. In [8] the surface energy is approximated by a crystalline one and a convergence analysis for the resulting scheme is given. A description of anisitropic motion by mean curvature in the context of Finsler geometry is given in [1] and [10] gives a survey of various mathematical approaches to (1). We finally note that the above techniques can be used in order to analyze a finite element scheme to approximate graph solutions of anisotropic surface diffusion, see [4].

REFERENCES

[1] G. Bellettini, M. Paolini, *Anisotropic motion by mean curvature in the context of Finsler geometry*, Hokkaido Math. J. **25** (1996), 537-566.

[2] K. Deckelnick, G. Dziuk, *Discrete anisotropic curvature flow of graphs*, Math. Modelling Numer. Anal. **33** (1999), 1203–1222.

[3] K. Deckelnick, G. Dziuk, *A fully discrete numerical scheme for weighted mean curvature flow*, Numer. Math. **91** (2002), 423–452.

[4] K. Deckelnick, G. Dziuk, C.M. Elliott, *Fully discrete finite element approximation for anisotropic surface diffusion of graphs*, SIAM J. Numer. Anal. **43** (2005), 1112–1138.

[5] C.M. Elliott, A. Gardiner, R. Schaetzle, *Crystalline curvature flow of a graph in variational setting*, Adv. Math. Sci. Appl. **8**(1) (1998), 425–460.

[6] F. Fierro, R. Goglione, M. Paolini, *Numerical simulations of mean curvature in the presence of nonconvex anisotropy*, Math. Models Methods Appl. Sci. **8**(4) (1998), 573–601.

[7] Y. Giga, *Motion of a graph by convexified energy*, Hokkaido Math. J. **23** (1994), 185–212.

[8] P.M. Girão, R.V. Kohn, *Convergence of a crystalline algorithm for the heat equation in one dimension and for the motion of a graph by weighted curvature*, Numer. Math. **67** (1994), 41–70.

[9] G.A. Lieberman, *The first initial–boundary value problem for quasilinear parabolic equations*, Ann. Sci. Norm. Sup. Pisa Ser. IV **8** (1986), 347–387.

[10] J.E. Taylor, J.W. Cahn, C.A. Handwerker, *Geometric models of crystal growth*, Acta metall. mater. **40** (1992), 1443–1474.

High-resolution flux-based level set method

Peter Frolkovic

(joint work with Karol Mikula)

New method for numerical solution of nonlinear degenerate level set equation will be presented. The method is formally second order accurate and consistent when applied with 2D/3D unstructured grids using different types of elements. It was implemented using a multilevel grid structure ("multi-grids") by applying a local refinement and coarsening of the computational mesh in time. The method is closely related to standard "flux-based" finite volume methods and can be implemented by relatively minor changes to existing codes for nonlinear advection-diffusion problems. Several 2D/3D examples will be shown involving ones with topological changes of the interface and with a grid adaptivity.

Dynamics of fluid vesicles with coexisting domains

Frank Hausser

(joint work with John Lowengrub, Andreas Rätz, Axel Voigt)

The strongly increasing interest in bilayer lipid membranes with coexisting fluid domains results from the hypothesized coupling of lipid phase segregation in the membrane to fundamental cell biological processes, such as membrane signaling and trafficing. Changes in lipid composition are assumed to assist or antagonize the membrane curvature on one side, but also might respond to the curvature by concentrating in domains of curvature that they prefer on the other side. Strong curvature variations have recently been observed experimentally in giant liposmes of relatively simple lipid compositions, where different lipids segregate according to their chemical properties and lead to the formation of buds and thus modify the membrane curvature locally. Subdomains of distinct curvature may have

precise biological properties, thus an understanding how lipid components can dynamically influence to membrane morphology is of utmost importance. With the curvature as one of the crucial incredicies to determine properties of membranes it seems natural to model the evolution within a continuum framework. This is further justified by the different length scales which come into play. The thickness of the bilayer is in the nanometerrange, while a typical size of a vesicle is in the micrometer range. This length scale separation allows the vesicle to be described as an elastic surface. The surface free energy is defined as $F[\Gamma, u] = F_B + F_S + F_T$ with

$$F_B[\Gamma, u] = \frac{1}{2} \int_\Gamma b_n(u)\big(H - H_0(u)\big)^2 d\Gamma + \int_\Gamma b_g(u) K d\Gamma \qquad \text{bending energy}$$

$$F_S[\Gamma, u] = \int_\Gamma \gamma(u) d\Gamma \qquad\qquad\qquad\qquad \text{excess energy}$$

$$F_T[\Gamma, u] = \int_\Gamma \frac{\delta^2}{2} |\nabla_\Gamma u|^2 + W(u) d\Gamma \qquad\qquad \text{line energy}$$

A thermodynamic consistend model can be derived from mass conservation and energy dissipation, see [1] and reads

$$\partial_t u + \nabla_\Gamma \cdot (u\mathbf{T}) + uVH - \nabla_\Gamma \cdot (\beta_u \nabla_\Gamma \frac{\delta F}{\delta u}) = 0$$

$$V = -\beta_v \big(\mathbf{n}\frac{\delta F}{\delta \Gamma} - uH\frac{\delta F}{\delta u}\big)\beta_u \nabla_\Gamma \frac{\delta F}{\delta u}$$

$$\mathbf{T} = -\beta_t \Big[\big(\mathbf{1} - \mathbf{n} \otimes \mathbf{n}\big)\frac{\delta F}{\delta \Gamma} + u\nabla_\Gamma \frac{\delta F}{\delta u}\Big].$$

This is a coupled system of 4th order equations, the evolution for the concentration u is of Cahn-Hilliard type and defined on an evolving surface, the evolution of the surface in normal direction is governed by a generalized Willmore flow and the tangential movement results from the last equation. In addition we require constraints on the volume and surface area. The area can be required to remain constant globally or locally. In either case the constraints are incorporated by Lagrange multipliers. For the local inextensibility constraint the governing equations modify to

$$V = V^u + \beta_V(\lambda^{vol} + H\lambda^{locarea})$$

$$\mathbf{T} = \mathbf{T}^u - \beta_T \nabla_\Gamma \lambda^{locarea}$$

the Lagrange multipliers are determined from

$$\frac{d}{dt} Vol(t) = \int_{\Gamma(t)} V\mathbf{n} d\Gamma = 0; \qquad HV + \nabla_\Gamma \cdot \mathbf{T} = 0.$$

Special parts of this highly nonlinear model have been considered numerically. In [2] the Cahn-Hiliard equation is solved on a stationary surface. Neglecting the concentration dependence, the Willmore flow with volume and local area constraints can be solved by modifying the parametric algorithm for Willmore flow introduced in [3]. Fig. 1 shows the evolution with and without constraints.
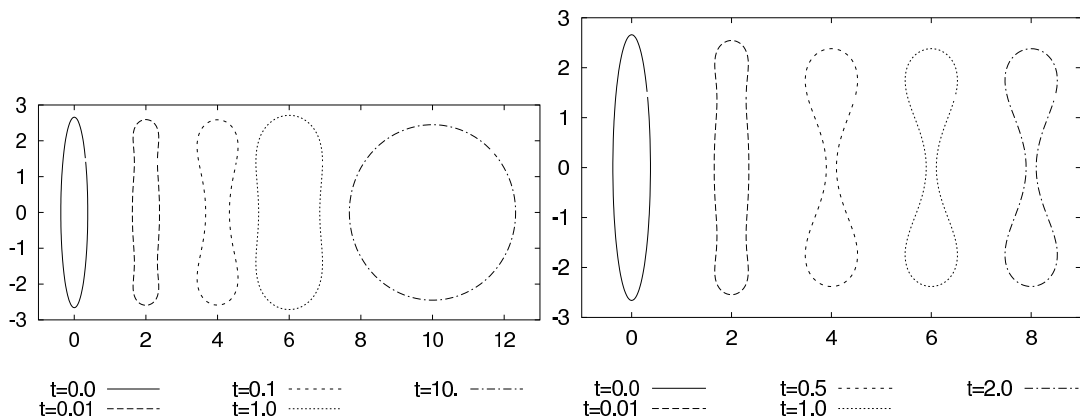
FIGURE 1. Evolution by Willmore flow without and with constraints on volume and local area.

REFERENCES

[1] F. Haußer, J. Lowengrub, A. Rätz, A. Voigt, (in preperation).
[2] A. Rätz, A. Voigt, *PDE's on surfaces - a diffise interface approach*, Comm. Math. Sci. (2006), .
[3] R. Rusu, , Interf. Free Bound. (2005), .

The anisotropic motion in human brains

CHIU-YEN KAO

(joint work with Marcel Jackowski, Lawrence Staib)

Determination of axonal pathways provides an invaluable means to study the connectivity of the human brain and its functional network. Diffusion tensor imaging (DTI) is unique in its ability to capture the restricted diffusion of water molecules which can be used to infer the directionality of tissue components. In this talk, a white matter tractography method based on anisotropic wavefront propagation in diffusion tensor images was introduced. A front propagates in the white matter with a speed profile governed by the isocontour of the diffusion tensor ellipsoid. By using the ellipsoid, we avoid possible misclassification of the principal eigenvector in oblate regions. The wavefront evolution is described by an anisotropic version of the static Hamilton-Jacobi equation, which is solved by a sweeping method in order to obtain correct arrival times. Pathways of connection are determined by tracing minimum-cost trajectories using the characteristic vector field of the resulting partial differential equation. Connectivity results using normal human DTI brain images are illustrated and discussed.

In the second half of the talk, we discuss the sweeping method based on the Lax-Friedrichs monotone numerical Hamiltonian to approximate viscosity solutions of arbitrary static Hamilton-Jacobi equations in any number of spatial dimensions. By using the Lax-Friedrichs numerical Hamiltonian, we can easily obtain the solution at a specific grid point in terms of its neighbors, so that a Gauss-Seidel

type nonlinear iterative method can be utilized. Furthermore, by incorporating a group-wise causality principle into the Gauss-Seidel iteration by following a finite group of characteristics, we have an easy-to-implement, sweeping-type, and fast convergent numerical method. However, unlike other methods based on the Godunov numerical Hamiltonian, some computational boundary conditions are needed in the implementation. We give a simple recipe which enforces a version of discrete min-max principle. Some convergence analysis is done for the one dimensional eikonal equation. Extensive 2-D and 3-D numerical examples in crystal growth and elastic waves illustrate the efficiency and accuracy of the approach.

Methods for computing and applications of the curve and surface evolution equations

Karol Mikula

In our talk we discussed a Lagrangean and Level-set approaches to solution of the geometrical partial differential equations and the application of the computational methods in real situations.

First we present Lagrangean computational methods, stabilized by tangential velocity functional, used for numerical solution of geometric equation $v = \beta(x, \nu, k, k_{ss})$ governing the motion of closed plane curves in the context of free boundary problems. The normal velocity v of an evolving curve may depend on its spatial position x, tangential angle ν, curvature k, and the intrinsic Laplacian of curvature k_{ss}. Such complex models appear, e.g., in thermodynamics with an anisotropic interfacial structure, in the elastic curve evolution in crystal growth, in the affine invariant multiscale shape analysis related to morphological image smoothing and in geodesic curvature flows on surfaces used in 2D digital image segmentation. We discuss suitable choices of tangential velocity and various examples of curve evolution with applications.

Next we present 2D and 3D semi-implicit complementary volume numerical scheme for solving Riemannian mean curvature flow of graphs and level sets applied to 2D and 3D image segmentation, edge detection, missing boundary completion and subjective contour extraction. We discuss level-set models leading to mean curvature driven image segmentation and outline basic advantages of the so-called subjective surface method given by the solution of the level-set equation

$$(1) \qquad u_t = \sqrt{\varepsilon^2 + |\nabla u|^2} \nabla . \left(g(|G * \nabla I^0|) \frac{\nabla u}{\sqrt{\varepsilon^2 + |\nabla u|^2}} \right),$$

where g is nonincreasing (so called Perona-Malik) function, $\varepsilon > 0$ and $G * \nabla I^0$ is a smoothed gradient of the segmented image. We present an experimental order of convergence of the method on nontrivial examples of exact solutions in case of the mean curvature motion in level-set formulation and discuss computational results related to biological and medical image segmentation.

The given results represent a joined works with Daniel Ševčovič and with S. Corsaro, A. Sarti and F. Sgallari.

REFERENCES

[1] S. CORSARO, K. MIKULA, A. SARTI, F. SGALLARI *Semi-implicit co-volume method in 3D image segmentation*, SIAM J. Sci. Comput., to appear in 2006

[2] A. HANDLOVIČOVÁ, K. MIKULA, F. SGALLARI, *Semi-implicit complementary volume scheme for solving level set like equations in image processing and curve evolution*, Numer. Math., 93 (2003) pp. 675–695.

[3] K. MIKULA, D. ŠEVČOVIČ, *Evolution of plane curves driven by a nonlinear function of curvature and anisotropy*, SIAM J. Appl. Math., 61 (2001) pp. 1473–1501.

[4] K. MIKULA, D. ŠEVČOVIČ, *Computational and qualitative aspects of evolution of curves driven by curvature and external force*, Computing and Visualization in Science, Vol. 6, No. 4 (2004) pp. 211-225.

[5] K. MIKULA, D. ŠEVČOVIČ, *Tangentially stabilized Lagrangian algorithm for elastic curve evolution driven by intrinsic Laplacian of curvature*, ALGORITMY 2005, Conference on Scientific Computing, Vysoke Tatry-Podbanske, Slovakia, March 13-18, 2005, Proceedings of contributed papers and posters (2005) pp. 32-41

[6] A. SARTI, R. MALLADI, J.A. SETHIAN, *Subjective Surfaces: A Method for Completing Missing Boundaries*, Proceedings of the National Academy of Sciences of the United States of America, Vol. 12, No. 97 (2000) pp. 6258-6263

Variational Approximation of Anisotropic Geometric Evolution Equations

ROBERT NÜRNBERG

(joint work with John W. Barrett, Harald Garcke)

We present a new variational formulation of both isotropic and fully anisotropic geometric evolution laws. Given a parameterization $\vec{x}(\rho, t) : \mathbb{R}/\mathbb{Z} \times [0, T] \to \mathbb{R}^2$ of the closed curve $\Gamma \subset \mathbb{R}^2$, we note that isotropic mean curvature flow and surface diffusion can be written as, respectively,

$$(1) \qquad \mathcal{V} := \vec{x}_t \,.\, \vec{\nu} = \begin{cases} \varkappa \\ -\Delta_s \, \varkappa \end{cases} \quad, \qquad \varkappa \vec{\nu} = \Delta_s \, \vec{x},$$

with $\varkappa$ the mean curvature of Γ and $\vec{\nu}$ a unit normal. Note that because the tangential component $\psi = \vec{x}_t \,.\, \vec{\tau}$ of the velocity $\vec{x}_t$ is not prescribed in (1), there exists a whole family of solutions $\vec{x}$, even though the evolution of Γ is uniquely determined.

On introducing the appropriate spaces $\underline{V}_0^h$ and W_0^h of periodic piecewise linear vector- and scalar-valued parametric finite elements, we propose the following approximation to (1), see [3, 2]. Find $\{\vec{X}^{m+1}, \kappa^{m+1}\} \in \underline{V}_0^h \times W_0^h$ such that

$$(2a) \qquad \langle \frac{\vec{X}^{m+1} - \vec{X}^m}{\tau_m}, \chi \, \vec{\nu}^m \rangle_m^h - \begin{cases} \langle \kappa^{m+1}, \chi \rangle_m^h \\ \langle \nabla_s \, \kappa^{m+1}, \nabla_s \, \chi \rangle_m \end{cases} = 0 \qquad \forall \, \chi \in W_0^h,$$

$$(2b) \qquad \langle \kappa^{m+1} \, \vec{\nu}^m, \vec{\eta} \rangle_m^h + \langle \nabla_s \, \vec{X}^{m+1}, \nabla_s \, \vec{\eta} \rangle_m = 0 \qquad \forall \, \vec{\eta} \in \underline{V}_0^h;$$

where $\langle f, g \rangle_m := \int_{\Gamma^m} f \,.\, g \; \mathrm{d}s = \int_{\mathbb{R}/\mathbb{Z}} f \,.\, g \, |\vec{X}_\rho^m| \, \mathrm{d}\rho$ with $\langle \cdot, \cdot \rangle_m^h$ the mass lumped inner product. It is now straightforward to show that there exists a unique solution

$\{\vec{X}^{m+1}, \kappa^{m+1}\} \in \underline{V}_0^h \times W_0^h$ to (2a,b). Moreover, the scheme (2a,b) is unconditionally stable. A remarkable feature of our method is, that it introduces a tangential velocity that redistributes the nodes in such a way, that they are eventually equidistributed. Although this cannot be shown for the fully discrete scheme (2a,b), this behaviour is observed in practice. Furthermore, it can be shown that a continuous in time semidiscrete version of (2a,b), as well as a fully discrete fully implicit version, equidistribute the vertices.

The approximation (2a,b) can be generalized to cover the geometric evolution of curve networks, where different curves move by their given normal velocities and where certain conditions have to hold at triple junctions, where three curves meet at a point. It turns out that the natural generalization of the weak formulation used to derive (2a,b) approximates all the necessary triple junction conditions correctly. Hence our parametric finite element approximation for the evolution of curve networks by mean curvature flow and surface diffusion, respectively, is given by (2a,b), with $\underline{V}_0^h$ and W_0^h replaced by the appropriate finite element spaces, and with $\langle f, g \rangle_m := \int_{\Gamma^m} f \cdot g \ \mathrm{d}s := \sum_{i=1}^{N_C} \int_{\Gamma_i^m} f_i \cdot g_i \ \mathrm{d}s$, where N_C is the number of curves.

Another advantage of our scheme (2a,b), that follows from the formulation (1), is that other evolution laws can be handled easily. For example, nonlinear mean curvature flow, $\mathcal{V} = f(\varkappa)$, including the inverse mean curvature flow, area preserving mean curvature flow, $\mathcal{V} = f(\varkappa) - \frac{\int_\Gamma f(\varkappa) \ \mathrm{d}s}{\int_\Gamma 1 \ \mathrm{d}s}$, Willmore flow for curves, $\mathcal{V} = -\Delta_s \varkappa - \frac{1}{2} \varkappa^3$, as well as an intermediate flow between area preserving mean curvature flow and surface diffusion, $\mathcal{V} = -\Delta_s (\frac{1}{\alpha} - \frac{1}{\xi} \Delta_s)^{-1} \varkappa$, can be approximated. All of these approximations will exhibit the equidistribution property of the scheme (2a,b).

Given an anisotropy function γ and an anisotropic mobility $\beta : S^1 \to \mathbb{R}_{>0}$, the fully anisotropic evolution equations corresponding to (1) are given by

$$(3) \qquad \vec{x}_t \cdot \vec{\nu} = \begin{cases} \beta(\vec{\nu}) \, \varkappa_\gamma \\ -\nabla_s \cdot (\beta(\vec{\nu}) \, \nabla_s \, \varkappa_\gamma) \end{cases} \quad , \qquad \varkappa_\gamma \, \vec{\nu} = [\gamma'(\vec{\nu})]_s^\perp \ ,$$

where $\varkappa_\gamma$ is the weighted mean curvature. A wide class of anisotropies can be modelled by

$$(4) \quad \gamma(\vec{p}) = \sum_{\ell=1}^L \gamma^{(\ell)}(\vec{p}) = \sum_{\ell=1}^L \sqrt{\vec{p} \cdot G^{(\ell)} \, \vec{p}} \qquad \Rightarrow \qquad \gamma'(\vec{p}) = \sum_{\ell=1}^L [\gamma^{(\ell)}(\vec{p})]^{-1} \, G^{(\ell)} \, \vec{p},$$

where $G^{(\ell)} \in \mathbb{R}^{2 \times 2}$, $\ell = 1 \to L$, are symmetric and positive definite; and we restrict our analysis to anisotropies of the form (4). This enables us to prove stability bounds for our fully discrete (parametric) approximations for anisotropic geometric evolution laws, see (5a,b) below, something that is new in the literature. We remark that variants of our proposed scheme can be used for anisotropies that are more general than (4), but it does not seem to be possible to prove analogue stability results in these more general situations.

On recalling the finite element spaces $\underline{V}_0^h$ and W_0^h, we propose the following approximation to (3), see [1]. Find $\{\vec{X}^{m+1}, \kappa_\gamma^{m+1}\} \in \underline{V}_0^h \times W_0^h$ such that

$$(5a) \quad \langle \frac{\vec{X}^{m+1} - \vec{X}^m}{\tau_m}, \chi\, \vec{\nu}^m \rangle_m^h - \begin{cases} \langle \beta(\vec{\nu}^m)\, \kappa_\gamma^{m+1}, \chi \rangle_m^h \\ \langle \beta(\vec{\nu}^m)\, \nabla_s \kappa_\gamma^{m+1}, \nabla_s \chi \rangle_m \end{cases} = 0 \qquad \forall\, \chi \in W_0^h,$$

$$(5b) \quad \langle \kappa_\gamma^{m+1}\, \vec{\nu}^m, \vec{\eta} \rangle_m^h + \sum_{\ell=1}^{L} \langle [\gamma^{(\ell)}(\vec{\nu}^m)]^{-1}\, G^{(\ell)}\, [\vec{X}_s^{m+1}]^\perp, \vec{\eta}_s^\perp \rangle_m = 0 \qquad \forall\, \vec{\eta} \in \underline{V}_0^h.$$

Note that for $\gamma(\vec{p}) = |\vec{p}|$ and $\beta \equiv 1$ the scheme (5a,b) collapses to the isotropic scheme (2a,b). As mentioned earlier, it is possible to show that the scheme (5a,b) is unconditionally stable. In addition, the scheme (5a,b) moves the vertices tangentially, so that the nodes are eventually equidistributed with respect to some nontrivial weighting function that depends on γ. Moreover, it is possible to approximate crystalline surface energies very accurately with (4). Hence one can use (5a,b) in order to simulate crystalline mean curvature flow as well as crystalline surface diffusion.

Finally, the scheme (5a,b) extends naturally to the anisotropic geometric evolution of curve networks. We are currently working on extending the ideas presented here to the isotropic and anisotropic evolution of hypersurfaces in $\mathbb{R}^3$.

REFERENCES

[1] J. W. Barrett, H. Garcke, and R. Nürnberg. Numerical approximation of anisotropic geometric evolution equations, 2006. Preprint No. 09/2006, University Regensburg.
[2] J. W. Barrett, H. Garcke, and R. Nürnberg. On the variational approximation of combined second and fourth order geometric evolution equations, 2006. Preprint No. 07/2006, University Regensburg.
[3] J. W. Barrett, H. Garcke, and R. Nürnberg. A parametric finite element method for fourth order geometric evolution equations. *J. Comput. Phys.*, 2006. (to appear).

A Variational Formulation for a Level Set Representation of Multiphase Flow and Area Preserving Curvature Flow

Peter Smereka
(joint work with Selim Esedoglu)

In this talk, variational descriptions for various level set formulations involving curvature flow are revisited. It is emphasized that a correct formulation requires one to consider all the level curves, not just the zero level set. This boils down to choosing the correct inner product for the gradient flow. Also discussed in this talk is the level set formulation of multiphase motion proposed by Zhao et al [1]. In their approach a separate level set function was associated to each phase. This required the introduction of a constraint to prevent vacuum formation and/or overlapping of phases. The authors then construct an energy functional in terms of the level set functions and include the constraint using Lagranges method. The Dirac delta functions that arise during the derivation of the Euler-Lagrange

equations are replaced by $|\nabla\phi|$ terms, a process Zhao et al call rescaling. A careful examination of this work reveals that the constraint actuals changes the normal velocity.

The talk given presents joint work in which a variational level set formulation for multiphase motion is given in which the constraint and the rescaling are removed. The main ideas are a novel representation of n phases using $n-1$ level set functions which has the advantage that the constraint which prevented overlapping or vacuum is not needed. In addition, by including the contribution of all level sets, not just the zero contour, in the energy functional and using the correct inner product one is able to produce a variational approach for a level set representation for multiphase flow. In addition, a variational formulation area preserving curvature flow is presented. In this flow the area (or volume) enclosed by each of the level sets is preserved. Each algorithm has been implemented numerically and the results of such computations are presented. The area preserving flow was successfully used for the super-resolution of images.

<div align="center">REFERENCES</div>

[1] H.K. Zhao, T.F. Chan, B. Merriman, S. Osher, *A variational level set approach to multiphase motion*, J. Comput. Phys. **127** (1996), 179-195.

<div align="center">

Towards a kinetic model for surface diffusion

AXEL VOIGT

(joint work with Lev Balykov, Frank Haußer, Andreas Rätz)

</div>

A classical interpretation of surface diffusion considers the H^{-1} gradient flow of a surface free energy. Let $\Gamma = \Gamma(t)$ be a compact smooth connected and oriented hypersurface in $I\!\!R^{d+1}$ and define $E[\Gamma] = \int_\Gamma \gamma \, d\Gamma$ as the surface free energy. If we define the chemical potential $\mu = \frac{\delta E}{\delta \Gamma}$, the surface flux $\mathbf{j} = -\nu\nabla_\Gamma\mu$, the evolution law reads $V = -\nabla_\Gamma \cdot \mathbf{j}$, with V being the normal component of the velocity. Different numerical approaches have been derived for this nonlinear 4th order equation, Fig. 1 shows the simulation results obtained with a parametric approach if $\gamma = 1$. In many applications the surface free energy density γ is a function of
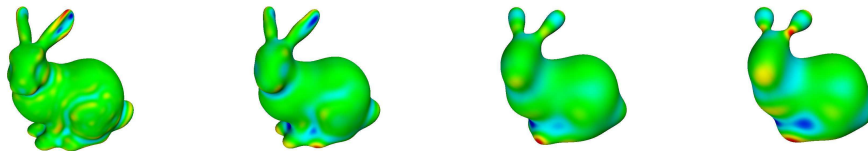

FIGURE 1. Surface diffusion on the Stanford bunny, surface mesh with ≈ 70.000 elements, see [1].

orientation. We consider convex and nonconvex functions. In the nonconvex case an additional higher order regularization by a Willmore functional is used, which

turns the surface diffusion model into a 6th order equation. Numerical approaches for this equation are discussed. For a graph formulation see [2], for a parametric setting see [3], for a level set approach see [4] and a phase-field approximations results from the following free energy

$$E[\phi] = \int_\Omega \frac{\epsilon}{2}|\gamma(n)\nabla\phi|^2 + \frac{1}{\epsilon}G(\phi)\ dx + \frac{\alpha^2}{2}\int_\Omega \frac{1}{\epsilon\gamma(n)}(-\epsilon\gamma(n)\Delta\phi + \frac{1}{\epsilon\gamma(n)}G'(\phi))^2\ dx$$

with ϕ being the phase-field variable, $G(\phi)$ a double well potential, ϵ the diffuse inteface width and α a new length scale over which corners are smeared out, see [5].

Non of these approaches considers kinetic effects. To incorporate kinetics associated with the rearrangement of atoms on the surface the model has to be modified. We define $\mu = \frac{\delta E}{\delta\Gamma} + bV$, with b a kinetic coefficient. Even if the equilibrium shape does not change, the pathway towards the equilibrium significantly differs if $b \neq 0$. For a comparison with non nonconvex γ see [6]. The actual quantities responsible for changes in the surface morphology, however are still not considered. On a microscopic picture, the surface changes due to attachment and detachment of free adatoms on surface defects. Models which include these free adatoms are only derived recently, see [7] and can be interpreted as a diffusion equation on an evolving surface, were the evolution is governed by a modified mean curvature flow.

$$\partial_t u + V + uHV = \Delta_\Gamma\mu$$

$$bV + \frac{\delta E}{\delta\Gamma} - \mu - uH\mu = 0,$$

with u the adatom concentration. The chemical potential μ is now defined as $\mu = \partial_u\gamma(u)$. A phase field approximation can be derived from the following energy

$$(1) \qquad\qquad E[\phi, u] = \int_\Omega \left(\frac{\epsilon}{2}|\nabla\phi|^2 + \frac{1}{\epsilon}G(\phi)\right)\gamma(u)\ dx$$

see [8]. Numerical simulations indicate the presence of different time scales. On a fast time scale the adatom concentration adjusts to the local curvature, on a time scale comparable to models without adatoms, the morphology evolved towards its equilibrium shape, and on a slow time scale the adatom concentration and morphology adjusts to the global minimum.

The kinetic effects associated with the attachemnt and detachment of adatoms on surface defects are incorporated through the coefficient b. In contrast to the functional form of γ and ν, for which material specific quantities can be computed from microscopic models, such as MD or DFT, a material specific from for b is not directly available. Models which circumvent this difficulty, by combining continuum and atomistic models have been introduced in [9, 10, 11]. In these models all kinetic effects are considered in a mean field approach and the normal velocity follows directly from the convection of surface defects.

References

[1] S. Vey, A. Voigt, *AMDiS - adaptive multidimensional simulations*, Comput. Vis. Sci. (in press).

[2] M. Burger, *Numerical simulation of anisotropic surface diffusion with curvature-dependent energy*, J. Comput. Phys. **203** (2005), 602-625.

[3] F. Haußer, A. Voigt, *A discrete scheme for regularized anisotropic surface diffusion, a sixth order geometric evolution equation*, Interf. Free Bound. **7** (2005), 1-17.

[4] M. Burger, F. Haußer, C. Stöcker, A. Voigt, *A level set approach to anistropic flows with curvature regularization*, J. Comput. Phys. (in review) .

[5] J. Lowengrub, A. Voigt, S. Wise, (in preperation), .

[6] C. Stöcker, A. Voigt, *The effect of kinetics in the surface evolution of thin crystalline films*, J. Cryst. Growth (in review).

[7] E. Fried, M.E. Gurtin, *A unified treatment of evolving interfaces accounting for small deformations and atomic transport with emphasis on grain-boundaries and epitaxy*, Adv. Appl. Mech. **40** (2004), 1-177.

[8] A. Rätz, A. Voigt, *A diffuse-interface approximation for surface diffusion including adatoms*, Nonlin. (in review).

[9] L. Balykov, A. Voigt, *A kinetic model of step flow growth of* [100] *steps*, Phys. Rev. E **72** (2005), 022601.

[10] L. Balykov, A. Voigt, *A 2 + 1 dimensional terrace-step-kink model for epitaxial growth far from equilibrium*, SIAM Multi. Mod. Sim. **5** (2006), 45-61.

[11] L. Balykov, A. Voigt, *A kinetic model for step flow growth in molecular beam epitaxy*, Surf. Sci. **600** (2006), 3436-3445.

Simulation dislocation dynamics in thin films using level set method

Yang Xiang

(joint work with Jerry Quek, Yongwei Zhang, David J. Srolovitz, Chun Lu)

The control of the density and location of dislocations (line defects) in heteroepitaxial thin-film is very important in designing semiconductor-based electronic devices. We have developed a level set method based, three dimensional dislocation dynamics simulation method to describe the motion of dislocations in thin films. This method is based on the level set method for dislocation dynamics in bulk materials proposed by Xiang et al. [1]. The dislocation location is given by the intersection of the zero level sets of a pair of level set functions. This representation does not require discretization and tracking of the dislocation and therefore handles topological changes naturally. The simulation method incorporates the elastic interactions of the dislocations and the stress fields throughout the film and substrate. Using the above approach, various dislocation interactions within a thin film are simulated.

References

[1] S.S. Quek, Y. Xiang, Y.W. Zhang, D.J. Srolovitz, C. Lu, *A kinetic model for step flow growth in molecular beam epitaxy*, Acta Materialia **51** (2003), 5499-5518.

Reporter: Martin Burger and Axel Voigt

Participants

Prof. Giovanni Bellettini
Dipartimento di Matematica
Universita di Roma "Tor Vergata"
Via della Ricerca Scientif. 1
I-00133 Roma

Benjamin Berkels
Institut für Numerische Simulation
Universität Bonn
Nussallee 15
53115 Bonn

Prof. Dr. Martin Burger
Fachbereich 10 - Mathematik und
Informatik
Universität Münster
Einsteinstr. 62
48149 Münster

Prof. Dr. Hajdin Ceric
Institut für Miktroelektronik
Technische Universität Wien
Gußhausstr. 27-29
A-1040 Wien

Prof. Dr. Klaus Deckelnick
Institut für Analysis u. Numerik
Otto-von-Guericke-Universität
Magdeburg
Universitätsplatz 2
39106 Magdeburg

Prof. Dr. Charles M. Elliott
Department of Mathematics
University of Sussex
Falmer
GB-Brighton BN1 9RF

Dr. Peter Frolkovic
Interdisziplinäres Zentrum
für Wissenschaftliches Rechnen
Universität Heidelberg
Im Neuenheimer Feld 368
69120 Heidelberg

Dr. Frank Haußer
Crystal Growth Group
Research Center CAESAR
Ludwig-Erhard-Allee 2
53175 Bonn

Dr. Chiu-Yen Kao
Institute for Mathematics and its
Applications
University of Minnesota
400 Lind Hall, 207 Church St.
Minneapolis MN 55455
USA

Prof. Dr. John L. Lowengrub
Department of Mathematics
University of California at Irvine
Irvine, CA 92697-3875
USA

Prof. Dr. Karol Mikula
Department of Mathematics, SvF
Slovak University of Technology
Radlinskeho 11
81368 Bratislava
SLOVAKIA

Dr. Robert Nürnberg
Department of Mathematics
Imperial College London
Huxley Building
GB-London SW7 2AZ

Prof. Dr. Peter Smereka
Dept. of Mathematics
The University of Michigan
2074 East Hall
525 E. University Ave.
Ann Arbor, MI 48109-1109
USA

Prof. Dr. Yang Xiang
Department of Mathematics
University of Science a. Technology
Clear Water Bay
Kowloon
Hong Kong
HONG KONG

Priv.Doz.Dr. Axel Voigt
Crystal Growth Group
Research Center CAESAR
Ludwig-Erhard-Allee 2
53175 Bonn